Human Molecular Genetics, 2012, Vol. 21, No. 14 ***3215–3225***
doi:10.1093/hmg/dds155
Advance Access published on April 20, 2012

Human DJ-1 and its homologs are novel glyoxalases

Ju-young Lee[1], Jeeyeon Song[1], Kyu Kwon[1], Sumi Jang[1], Chayeon Kim[1], Kwanghee Baek[3], Jeongho Kim[2,*] and Chankyu Park[1,*]

[1]Department of Biological Sciences, Korea Advanced Institute of Science and Technology, Yuseong-gu, Daejeon 305-701, Republic of Korea, [2]Department of Biological Sciences, Inha University, Incheon 402-751, Republic of Korea and [3]Department of Genetic Engineering and Graduate School of Biotechnology, Kyung Hee University, Yongin 446-701, Republic of Korea

Received February 16, 2012; Revised March 29, 2012; Accepted April 12, 2012

Human DJ-1 is a genetic cause of early-onset Parkinson's disease (PD), although its biochemical function is unknown. We report here that human DJ-1 and its homologs of the mouse and *Caenorhabditis elegans* are novel types of glyoxalase, converting glyoxal or methylglyoxal to glycolic or lactic acid, respectively, in the absence of glutathione. Purified DJ-1 proteins exhibit typical Michaelis–Menten kinetics, which were abolished completely in the mutants of essential catalytic residues, consisting of cysteine and glutamic acid. The presence of DJ-1 protected mouse embryonic fibroblast and dopaminergically derived SH-SY5Y cells from treatments of glyoxals. Likewise, *C. elegans* lacking cDJR-1.1, a DJ-1 homolog expressed primarily in the intestine, protected worms from glyoxal-induced death. Sub-lethal doses of glyoxals caused significant degeneration of the dopaminergic neurons in *C. elegans* lacking cDJR-1.2, another DJ-1 homolog expressed primarily in the head region, including neurons. Our findings that DJ-1 serves as scavengers for reactive carbonyl species may provide a new insight into the causation of PD.

INTRODUCTION

DJ-1 is known as a genetic cause for the early-onset Parkinson's disease (PD) (1). Since its first discovery as an oncogene (2), various roles of this protein have been reported, primarily in protecting cells from oxidative stress (3,4) and exerting neuroprotection against PD-causing agents, such as MPP^+, 6-OHDA and rotenone (5–7). Although DJ-1 and its homologs have been primarily implicated in oxidative stress, its precise biochemical mechanism remains unknown. The protective effects of DJ-1 against oxidative stress were demonstrated in various species, including mammalian cells (3), *Drosophila melanogaster* (5) and *Caenorhabditis elegans* (8,9). For *C. elegans* DJ-1, a knockdown study was carried out to demonstrate that the animal exhibited an increased vulnerability to rotenone, which was rescued by antioxidants (8).

α-Oxoaldehydes including glyoxal (GO) and methylglyoxal (MGO) are produced by glucose oxidation, lipid peroxidation and DNA oxidation (10). They react non-enzymatically with amino groups of proteins, forming advanced glycation end-products (AGEs), which were implicated in aging, diabetes and neurodegenerative diseases, such as Parkinson and Alzheimer (11–13), as well as in apoptosis of cells, including neurons (14). These reactive electrophiles are known to be removed by the glutathione-dependent glyoxalase (GLO I and II) (15) and NAD[P]H-dependent aldo-keto reductase (AKR) (16). A novel type of glyoxalase, named Glo III, has been reported in *Escherichia coli* (17), converting methylglyoxal into lactic acid in the absence of any co-factor. Recently, we characterized the product of the *E. coli hchA* gene as glyoxalase III, which is also a remote member of DJ-1 superfamily (18). Here, we characterized human DJ-1 and its homologs in the mouse and *C. elegans* as glyoxalases and investigate their roles in protecting cells, neurons and worms from glyoxals. The presence of DJ-1 enzymes enhanced cell and worm viabilities when exposed to these oxoaldehydes, and in particular protected dopaminergic neurons from their toxicities.

*To whom correspondence should be addressed. Tel: +82 423502629; Fax: +82 423504240; Email: ckpark@kaist.ac.kr (C.P.); Tel: +82 328607691; Fax:+82 328746737; Email: jhokim@inha.ac.kr (J.K.)

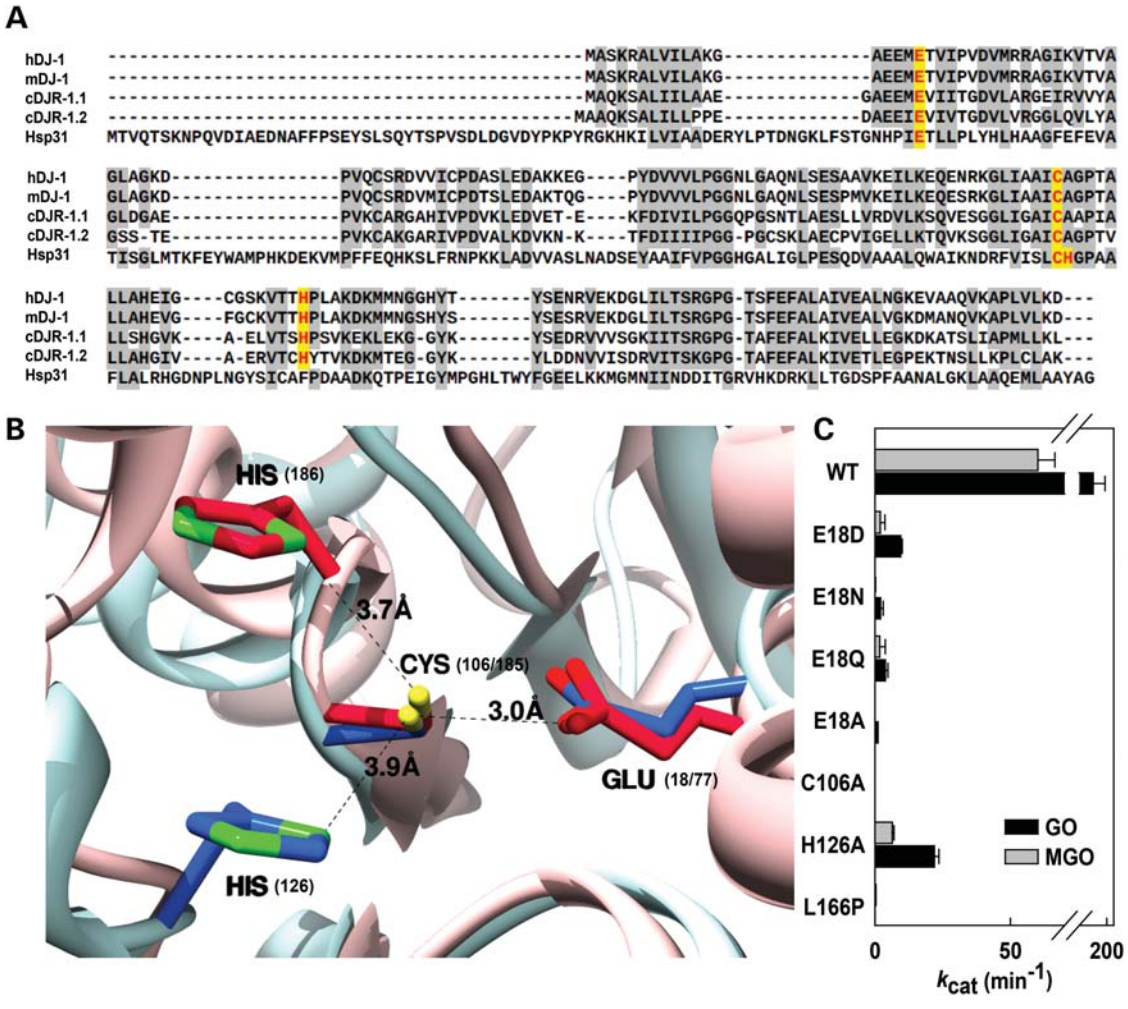

Figure 1. Comparison of sequence and structure between DJ-1 and its homologs. (**A**) Comparison of amino acid sequences (Clustal W) between human, mouse, *C. elegans* and *E. coli* DJ-1 homologs. Three predicted catalytic residues are highlighted. (**B**) Molecular models drawn with Chimera (www.cgl.ucsf.edu/chimera). The X-ray structure of human DJ-1 (blue) is superimposed with the structure of *E. coli* HchA (red), with their catalytic residues marked. Distances between the residues are also presented. (**C**) Enzyme activities of WT and mutant DJ-1s. K_{cat} values for GO and MGO were measured with DNPH assay, using 50 μg (WT) and 100 μg (mutants) of purified proteins.

RESULTS

Human DJ-1 and its homologs are glyoxalases

The bacterial glyoxalase III (HchA protein) shares a homology with the DJ-1 subfamily proteins in its major catalytic domain, although the bacterial enzyme contains an extra domain surrounding the active site (19). Although the human/mouse DJ-1 and *C. elegans* homologs are somewhat diverged from their bacterial counterpart in both the sequence and structure, the catalytic residues of histidine, cysteine and glutamic acid (18) are always found in the presumed active site (Fig. 1A and B). The structures of mDJ-1, cDJR-1.1 and cDJR-1.2 were obtained based on homology modeling (Supplementary Material, Fig. S1). Even though the bacterial and animal enzymes contain the three catalytic residues, they are not conserved in the primary sequences. Rather, they seem to be arisen independently during their lineages, especially the histidine residues. Based on the recent characterization of the bacterial enzyme, we carried out an experiment for animal enzymes to determine whether they exhibit glyoxalase activities. The His-tagged hDJ-1, mDJ-1, cDJR-1.1 and cDJR-1.2 were purified using the Ni-affinity column and were used to determine the enzymatic activity and conditions for the catalytic reaction (Materials and Methods, Supplementary Material, Fig. S2). The results show typical Michaelis–Menten kinetics for all the enzymes tested (Fig. 2B and D, Supplementary Material, Table S1). The reaction products were identified by ^{1}H-NMR and high-performance liquid chromatography (HPLC), such that lactic and glycolic acids were produced from methylglyoxal and glyoxal, respectively (Fig. 2A and C). Various types of aldehydes, including acetaldehyde, acrolein, glyceraldehydes, 2,3-butanedione and 2-carboxybenzaldehyde, were also tested as substrates, in which none of them was shown to be positive (unpublished data). The DJ-1 homologs have in general slightly higher affinities to methylglyoxal than to glyoxal, while specific activities are higher for glyoxal than for methylglyoxal (Table 1). Although the DJ-1 proteins react with phenylglyoxal, a synthetic substrate, 3-deoxyglucosone did not serve as a substrate (unpublished data).

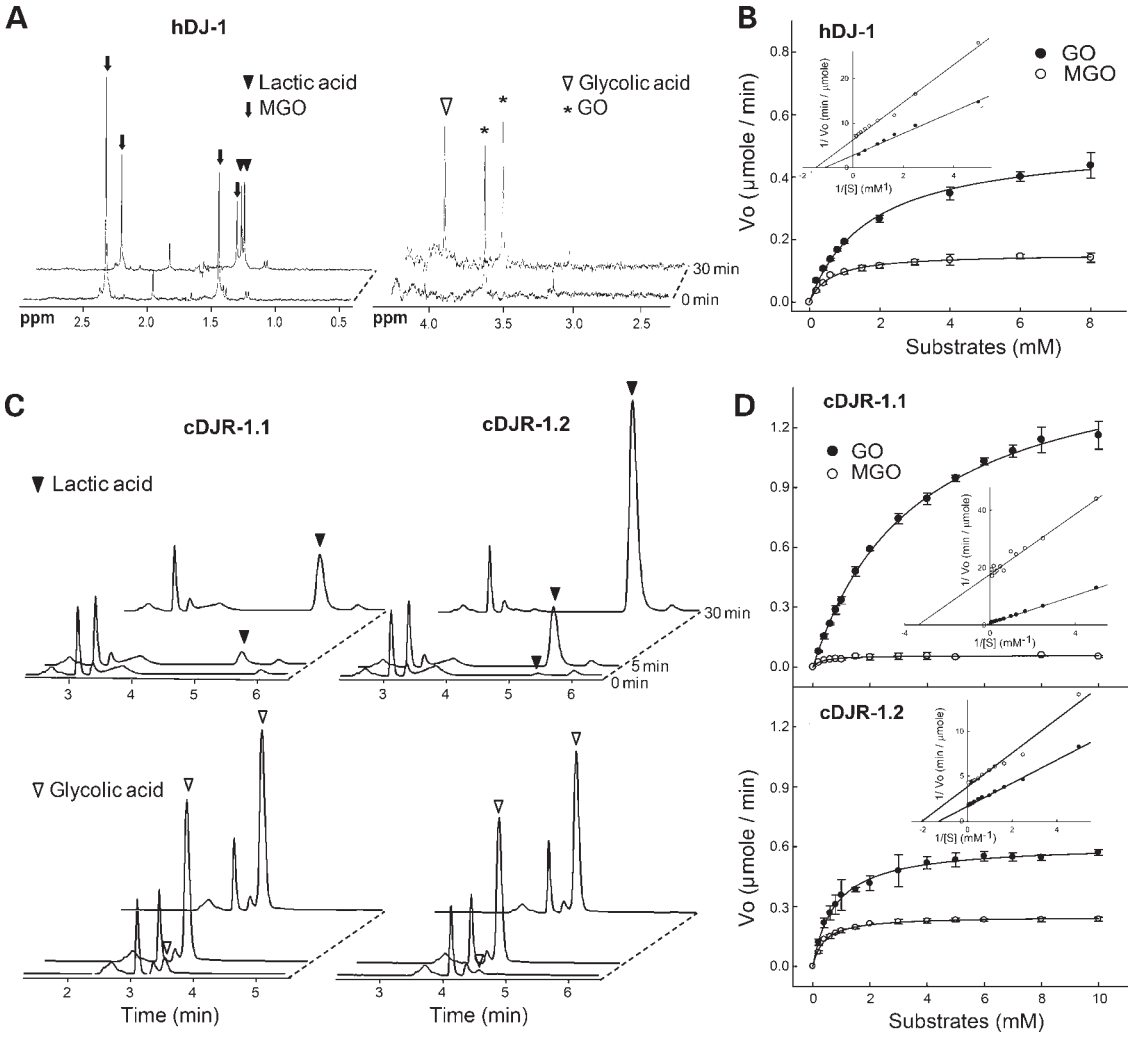

Figure 2. Characterization of the DJ-1 homologs as glyoxalases. (**A**) Purified human DJ-1 (50 μg) was mixed with GO (5 mM) or MGO (3 mM) for 30 min, and their reaction products, glycolic acid and lactic acid (two peaks), respectively, were analyzed with NMR. The peak appeared at ∼2 ppm is acetate contained in the reagent from Sigma, and (*) indicates ethylene glycol, a contaminant. (**B**) The glyoxalase reaction of DJ-1 was also analyzed with DNPH assay, from which initial velocities were plotted with Michaelis–Menten and Lineweaver–Burk (inset) equations. Error bars represent standard deviations with triplicate experiments. (**C**) Purified DJ-1s from *C. elegans* were mixed with GO (10 mM) or MGO (10 mM), from which glycolic and lactic acids were detected by HPLC. The products were formed proportional to reaction time. (**D**) Enzyme reactions with cDJR-1.1 (100 μg) and cDJR-1.2 (100 μg) were monitored and plotted as described in (**B**).

Since the animal DJ-1 homologs have similar catalytic structures to that of the bacterial enzyme (18), we undertook an approach to mutate these residues and see whether they play the same catalytic roles. The human DJ-1 proteins with E18A, E18D, E18N, E18Q, C106A and H126A mutations were purified and tested for their abilities to convert glyoxals (Fig. 1C). As in the case of the bacterial enzyme, the changes in invariant cysteine and glutamic acid completely removed the enzyme activity, whereas the histidine change left some amount (ca. 10%) of enzyme activity. We also generated a mutation of L166P found in familial Parkinsonism, which exhibits significant defect in glyoxalase activity. The C106S mutation in cDJR-1.1 also completely abolished its enzymatic activity (Table 2), confirming the essential role of cysteine in glyoxalase.

The novel glyoxalase characterized here appears to be the only cofactor-independent enzyme in animals as in *E. coli*, since the removal of *djr-1.1* and/or *djr-1.2* genes in *C. elegans* from the wild-type (WT) N2 worms eliminate glyoxalase activity, which were rescued in *djr-1.1* or *djr-1.2* transgenic worms (Table 2); the loss of cDJR-1.1 decreased ∼71% of the enzyme activity for GO and the loss of cDJR-1.2 decreased ∼28%. The same is true for the mouse (Table 2), in which crude brain extracts of knockout mice did not show significant activities for converting glyoxal to glycolic acid. In our initial attempt to purify co-factor independent enzyme from mouse liver (Supplementary Material, Table S2), such activity was strongly correlated with the presence of mDJ-1 that was monitored by immunoblot (unpublished data), again suggesting mDJ-1 as the sole glyoxalase. Previously, it was reported that human blood plasma contains some amount of glyoxal, ca. 1.15 ± 0.34 μM (20). When we measured the levels of free glyoxal in the mouse and *C. elegans*, they were estimated to be 1.11 ± 0.14 (WT)

Table 1. Enzymatic constants for purified DJ-1s

Type	Methylglyoxal K_m (mM)	k_{cat} (min^{-1})	k_{cat}/K_m (min^{-1} M^{-1})	Glyoxal K_m (mM)	k_{cat} (min^{-1})	k_{cat}/K_m ($min^{-1}M^{-1}$)
hDJ-1	0.60	72.38	1.21×10^5	1.39	199.3	1.43×10^5
mDJ-1	0.84	53.8	0.64×10^5	1.48	184.0	1.24×10^5
cDJR-1.1	0.30	13.8	0.46×10^4	3.61	356.4	0.99×10^5
cDJR-1.2	0.39	60.0	1.53×10^5	0.78	146.4	1.88×10^5

and 1.12 ± 0.15 μM (DJ-1 KO) in mouse brain, and 2.31 ± 0.30 (WT) and 3.20 ± 0.38 μM (DJR KO) in *C. elegans*, implying that cells accumulate some amount of glyoxals, even though they are constantly detoxified by glyoxalase I/II and AKR (e.g. mAKR 1B3), requiring glutathione and nicotinamide adenine dinucleotide phosphate (NADPH) for their activities, respectively. Previously, compensatory induction of glyoxalase I was noted for α-synuclein knockout mice (21), and the enzyme was shown to be down-regulated in Nrf2 knockout mice (22), in which Nrf2 was presumably stabilized by DJ-1 (23). However, we observed that the activity of glyoxalase I in the mouse was essentially unchanged regardless of the presence of DJ-1; 99.3 ± 1.3 and 100.0 ± 1.9 unit/μg protein in the WT and mDJ-1 knockout brains, respectively. When we assessed the relative contribution of DJ-1 in scavenging glyoxal in mouse brain and *C. elegans* extracts, we found considerably higher proportion of DJ-1 enzymes in the worm (ca. 40%) than in the mouse (ca. 8%, unpublished data). This may explain why we were able to observe an increase in the steady-state level of glyoxal in DJR knockout worms relative to that of the WT, although the DJ-1 knockout in the mouse does not significantly alter the glyoxal level.

Expression patterns of the DJ-1 proteins

Mammals contain a single DJ-1 homolog, while *C. elegans* has two isoforms. Previous studies indicate that the DJ-1 protein is ubiquitously distributed in all types of tissues (http://biogps.org). Expressions in tissues including the heart, skeletal muscles, pancreas, liver, testis and brain were reported in the human by northern blot analysis (2,24). It was also reported that DJ-1 is highly expressed in the substantia nigra and the frontal cortex (25). A similar pattern of DJ-1 expression was observed in the mouse, especially in the hippocampus, cerebral cortex and substantia nigra (26). We observed considerable variation in mDJ-1 expressions, significantly higher in the brain and liver relative to that of the embryonic fibroblast (unpublished data).

To understand the function of DJ-1 homologs in *C. elegans*, we first examined localizations of expressions in transgenic worms carrying a green fluorescent protein (GFP) fusion construct to the promoter regions of *djr-1.1* or *djr-1.2* ($P_{djr-1.1}$::*djr-1.1*::*gfp* and $P_{djr-1.2}$:: *gfp*::*djr-1.2*). Expression of cDJR-1.1::GFP was detected exclusively in the intestine, while GFP::cDJR-1.2 was expressed in various tissues, including pharyngeal muscles, pharynx-intestinal valve, ventral nerve cord, spermatheca, rectal gland, inner labial (IL) cells of head neurons, phasmid (PHA/PHB) neurons in tail and supporting sheath/socket cells throughout the whole stages of worms (Fig. 3A). Additional expression of cDJR-1.2 in head-mesodermal cell (HMC), excretory canals and coelomocytes was also observed in 5-day adult stages (Fig. 3B). Since DJ-1 has been implicated in PD, we examined whether cDJRs are expressed in dopaminergic neurons. When we generated a transgenic line carrying both dopaminergic neuronal marker P_{dat-1}::mCherry and GFP::cDJR-1.2, we did not observe cDJR-1.2 expression in a detectable amount in any of the eight dopaminergic neurons (CEPs, ADEs and PDEs, unpublished data). The major expression sites of cDJR-1.1 and cDJR-1.2 do not overlap and are fairly consistent throughout the whole larval and adult stages of worms. When we examined the subcellular localization of cDJRs, cDJR-1.1 was found in both the nucleus and cytoplasm of the intestinal cells, whereas cDJR-1.2 was detected only in the cytosol of head neurons (Fig. 3C). These localization patterns of cDJRs were consistent with those of COS-7 cells transfected with Flag-tagged cDJRs, confirmed by immunostaining with anti-Flag antiserum conjugated with fluorescein isothiocyanate (FITC), as well as by cell fractionation (Fig. 3D–E). cDJR-1.1 was ubiquitously localized throughout the whole cells with higher expression in the nucleus, while cDJR-1.2 was only present in the cytoplasm, which was also confirmed with enhanced green fluorescent protein-cDJR (Supplementary Material, Fig. S3).

Roles of DJ-1 in protecting cells and worms from glyoxal-induced death

We prepared mouse embryonic fibroblast (MEF) cells from the DJ-1 knockout mouse and generated derivatives stably expressing WT or mutant hDJ-1s under the viral promoter, since the mDJ-1 expression in MEF is quite low. When we treated glyoxal for mDJ-1 knockout MEFs carrying the WT and catalytic mutant forms of hDJ-1s, we observed significant protection of cells containing the WT DJ-1 from glyoxal, thereby enhancing cell viability (ca. 63%) compared with those of knockout and catalytic mutants (Fig. 4A). Similar protection of dopaminergic neuronal cells (SH-SY5Y) from human was observed with stably expressed human DJ-1 compared with that of the vector control. The presence of additional DJ-1 in SH-SY5Y cell increased protection to glyoxal, with >45% of cell survival. The protection by DJ-1 appears to be specific for glyoxals, since the treatments with other types of aldehydes have nothing to do with the presence of DJ-1 (Supplementary Material, Fig. S4). α-Oxoaldehydes were previously shown to induce apoptosis in neuronal cells (14), so that we tested whether DJ-1 protects neurons from glyoxal-induced apoptosis (Fig. 4B). As shown in Figure 4B, an increase in the PARP-1 cleavage was observed in cells with less DJ-1 relative to that of cells with more DJ-1, so does the increase in phosphorylation of p38.

Table 2. Specific activities of glyoxalase in mouse and worm

Genotype	Activity[a] (unit/μg protein)
M. musculus C57B/6	
WT brain	8.82 ± 0.99
mDJ-1$^{-/-}$ brain	n.d.
C. elegans N2	
WT	7.23 ± 0.26
djr-1.1	2.23 ± 0.34*
djr-1.2	5.28 ± 0.35
djr-1.1;1.2	n.d.
djr-1.1;1.2 + P$_{djr-1.1}$::*djr-1.1*::*gfp*	4.92 ± 0.29
djr-1.1;1.2 + P$_{djr-1.1}$::*djr-1.1*(*C106S*)::*gfp*	n.d.
djr-1.1;1.2 + P$_{djr-1.2}$::*gfp*::*djr-1.2*	3.10 ± 0.92

[a]Enzyme activity for mouse tissues were measured with 10 mM GO at 37°C by DNPH assay, and worm extracts with 10 mM GO at 22°C by DNPH assay. Buffer conditions were 100 mM Na_3PO_4, pH 7.4. Values indicate mean and SD with triplicate experiments.
n.d.: not detectable.
*$P < 0.005$, *t*-test.

The results imply that the protection from glyoxal by DJ-1 is due to the reduction in apoptotic signaling, presumably by lowering intracellular levels of glyoxals.

In order to test the possibility that the glyoxal-induced death is associated with oxidative stress, we observed SH-SY5Y cells for an increase in reactive oxygen species (ROS) with CM-DCF fluorescence (Supplementary Material, Fig. S5). The results show very little increase in fluorescence upon glyoxal treatment compared with that of the hydrogen peroxide-treated control. The glyoxal-induced death resulted in an accumulation of Nε-carboxymethyl lysine (CML), the glycated protein, which disappears with an addition of aminoguanidine (AG), the compound specifically reacting with glyoxals (Fig. 4B). On the other hand, deaths of SH-SY5Y cells with hydrogen peroxide were neither protected by AG nor accompanied by an accumulation of CML-containing proteins, suggesting that glyoxal-induced death is unlikely to involve the change in ROS.

The role of DJ-1 in protecting cells from glyoxals was also assessed in *C. elegans* by carrying out a survival assay after treatment of worms with GO or MGO (Fig. 4C). The *djr-1.1* mutant showed decreased viability compared with that of the WT, while the effect of glyoxal in *djr-1.2* mutants was slightly less, implying that cDJR-1.1 plays a primary role in protecting worms from these aldehyde compounds. The importance of cDJR-1.1 was further substantiated by the fact that rescuing only *djr-1.1* in *djr-1.1 djr-1.2* double-mutant worms was able to exert protection against glyoxals, close to the WT level. The catalytic mutant of cDJR-1.1 (C106S) failed to rescue the phenotype of double mutants in terms of glyoxal-induced death, indicating that the glyoxalase activity itself is critical in *C. elegans*. On the other hand, the transgenic expression of GFP::cDJR-1.2 did not significantly increase the protective effect, suggesting that the location and abundance of cDJR-1.1 relative to that of cDJR-1.2 (Fig. 3) may justify its major role in glyoxal detoxification. Removal of *djr-1.1* and/or *djr-1.2* genes from the WT did not affect their lifespans (17–18 days, Supplementary Material, Fig. S6A), implying that the cDJRs may not serve as a primary scavenger for glyoxals, since the knockdown of glyoxalase I was reported to reduce lifespan (27). Rather, the cDJRs might have other regulatory roles in response to intracellular changes of glyoxal levels.

Glyoxals cause neuronal degeneration in *C. elegans* that is ameliorated by cDJRs

DJ-1 is known to protect dopaminergic neurons from chemicals causing PD. In *C. elegans*, there are eight dopaminergic neurons, including four cephalic (CEP) neurons, two anterior deirid (ADE) neurons and two posterior deirid (PDE) neurons (9). It is well known that 6-hydroxydopamine (6-OHDA), a neurotoxin that can specifically affect dopaminergic neurons, causes degeneration of these neurons with higher sensitivity to CEP neurons (28). Neurons exhibit morphological changes of blebbing, cell body rounding and eventual loss of cells. We observed similar dose-dependent degeneration of CEP neurons when treated worms with glyoxal or methylglyoxal (Supplementary Material, Fig. S7). The characteristic loss of dopaminergic neurons was monitored with transgenic worms containing dopaminergic neuronal marker P$_{dat-1}$::mCherry, showing progressive changes of blebbing and cell body loss (Fig. 5A). When larval worms from WT and mutants were treated with 50 mM GO or 20 mM MGO, respectively, the significant loss (>20%) of intact CEP was observed in *djr-1.2* and *djr-1.1*;*djr-1.2* strains compared with that of the WT (Fig. 5B). The GFP::cDJR-1.2 transgenic worms derived from *djr-1.1*;*djr-1.2* restored neuronal survival to the WT level. Since the role of cDJR-1.1 in protecting CEP dopaminergic neuron was negligible, we did not test the glyoxal effect for the *djr-1.1* rescue construct in *djr-1.1;djr-1.2* mutant worms. Under the same conditions without glyoxals, mutants lacking cDJR-1.1/1.2 did not show any difference in CEP viability compared with that of the WT (unpublished data). The loss of CEP neurons observed with sub-lethal concentrations of glyoxals indicates a neuronal susceptibility to these chemicals, which can be protected by cDJR-1.2 exerting detoxification activity. In order to test whether *djr-1.2* protects other neurons, we generated a transgenic line containing P$_{srb-6}$::mCherry that was used to visualize ASH and ADL, 2 of the 12 chemosensory neurons located in the anterior region of the pharynx. Treatment of glyoxals also resulted in progressive changes of dendrite blebbing and cell body loss of these neurons (Fig. 5C), suggesting that the neurotoxicity of glyoxals is not specific to dopaminergic neurons. However, cDJR-1.2 failed to protect these neurons upon glyoxal treatment (Fig. 5D), suggesting that the neuroprotective activity of cDJR-1.2 is not effective in all types of neurons, but rather likely to be specific in dopaminergic neurons.

DISCUSSION

Detoxifying reactive α-oxoaldehydes is crucial, since accumulation of these metabolites exerts deleterious effects on cellular macromolecules such as nucleic acids and proteins, leading to an accumulation of toxic AGEs (10,12). Moreover, α-oxoaldehydes are associated with decrease in GSH (29),

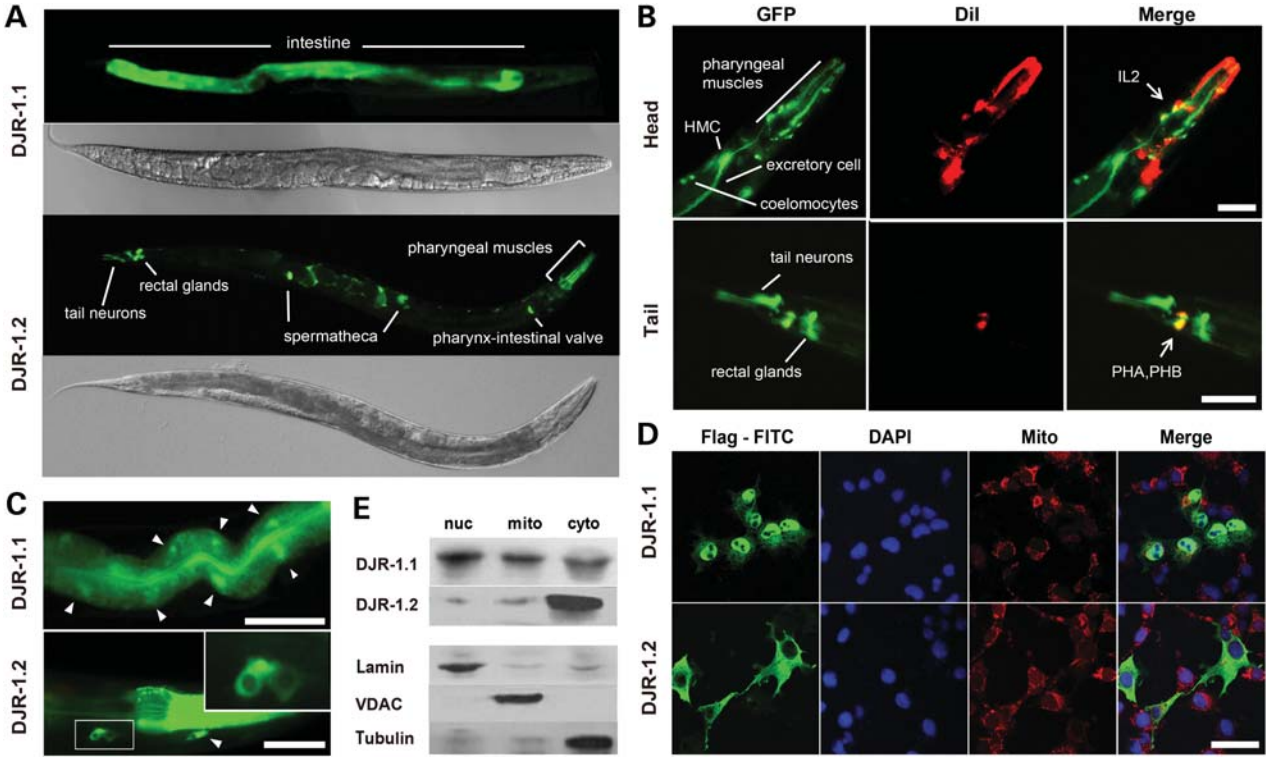

Figure 3. Tissue-specific localizations of cDJR-1.1 and cDJR-1.2. (**A**) cDJR-1.1::GFP was detected in the whole intestine of young adult worms, while GFP::cDJR-1.2 expression was found in the ventral nerve cord, pharyngeal muscles, head neurons, pharynx-intestinal valve, spermatheca, rectal glands and tail neurons including PHA and PHB. (**B**) Five-day adult worms show additional cDJR-1.2 expression in HMC, coelomocytes and excretory cell. Additional DiI staining with 50 mM calcium acetate shows that cDJR-1.2 is expressed in IL2 (head) and PHA/PHB (tail) neurons. (**C**–**E**) Subcellular localizations of cDJR-1.1 and cDJR-1.2 were examined by expressing GFP-tagged cDJR-1.1 and cDJR-1.2. (C) cDJR-1.1 is ubiquitously expressed throughout intestinal cells with higher intensity in nucleus (arrowheads), whereas cDJR-1.2 is expressed in the cytoplasm of head neurons (arrowheads). Scale bars = 40 μm. (D) COS7 cells expressing flag-tagged *djr-1.1* or *djr-1.2* were immunostained and visualized with confocal microscopy, showing similar results. Scale bars = 0.05 μm. (E) Subcellular expression levels of cDJRs were also confirmed by western blotting, in which 20 μg proteins of cell fractions were loaded.

induction of apoptosis (30) and disease progression, e.g. diabetes (12). Earlier studies on PD suggested an accumulation of intracellular glyoxals as a cause of neurodegenerative diseases (11). Although glyoxalase I/II and AKRs are well known for removing α-oxoaldehydes, severe or prolonged exposure of cells to such chemicals causes abnormality in the function of detoxifying enzymes, presumably due to depletion of glutathione or NADPH (27). Reports on elevated glutathione levels in DJ-1 overexpressing cells (31) may support the role of DJ-1 as a glyoxalase, scavenging α-oxoaldehydes. The evolutionary conservation of glyoxalase enzymes in diverse species including human, *C. elegans* and bacteria (18) is apparent from their structural homology, conserved catalytic residues and the presence of cysteine as a crucial residue for enzymatic activity (Figs 1 and 4). Generalization of glyoxalase function in DJ-1 superfamily proteins awaits further experiments to determine their enzymatic specificities. For example, the *E. coli* YajL protein, the closest bacterial homolog of human DJ-1 (32), did not show activity to methylglyoxal (5–10 mM, J.-y.L. and C.P., unpublished data), although unlike HchA their dimeric structures are very much alike. On the other hand, DJ-1β of *D. melanogaster*, containing a tyrosine instead of the catalytic histidine in its predicted three-dimensional structure (http://swissmodel.expasy.org), exhibits normal level of glyoxalase activity even with a mutation in the tyrosine residue (Supplementary Material, Table S1).

Caenorhabditis elegans cDJR-1.2 was shown to have significant protective effects against GO and MGO in CEP neurons (Fig. 5), and also on 6-OHDA (ca. 20%, Supplementary Material, Fig. S8), indicating that *C. elegans* cDJR-1.2 exerts neuro-protective effects, as in the mammalian DJ-1 (30,33). This result may be due to high expression of cDJR-1.2 in IL-2 IL neurons and some other neuron-supporting glial cells in the head region. It is uncertain whether CEP death is due to an absence of DJ-1 in the dopaminergic neuron itself, albeit undetectable with the GFP fusion, or due to misfunction of other supporting cells, including glial cells. The protection of CEP neurons by cDJR-1.2 might be due to its catalytic role reducing local concentration of glyoxal in the head region. As a matter of fact, some effects of cDJR-1.2 on glycation of cellular proteins were detected when we treated WT and Δ*djr-1.2* worms with GO that was subject to western blot analysis using anti-Nε-CML antiserum (Supplementary Material, Fig. S6B). The absence of cDJR-1.2 considerably increased CML, which is even higher than that of worms lacking cDJR-1.1.

Previous reports indicate that DJ-1 preferentially protects dopaminergic neurons upon oxidative stress (7,34). The exact relationship between oxidative stress condition and the

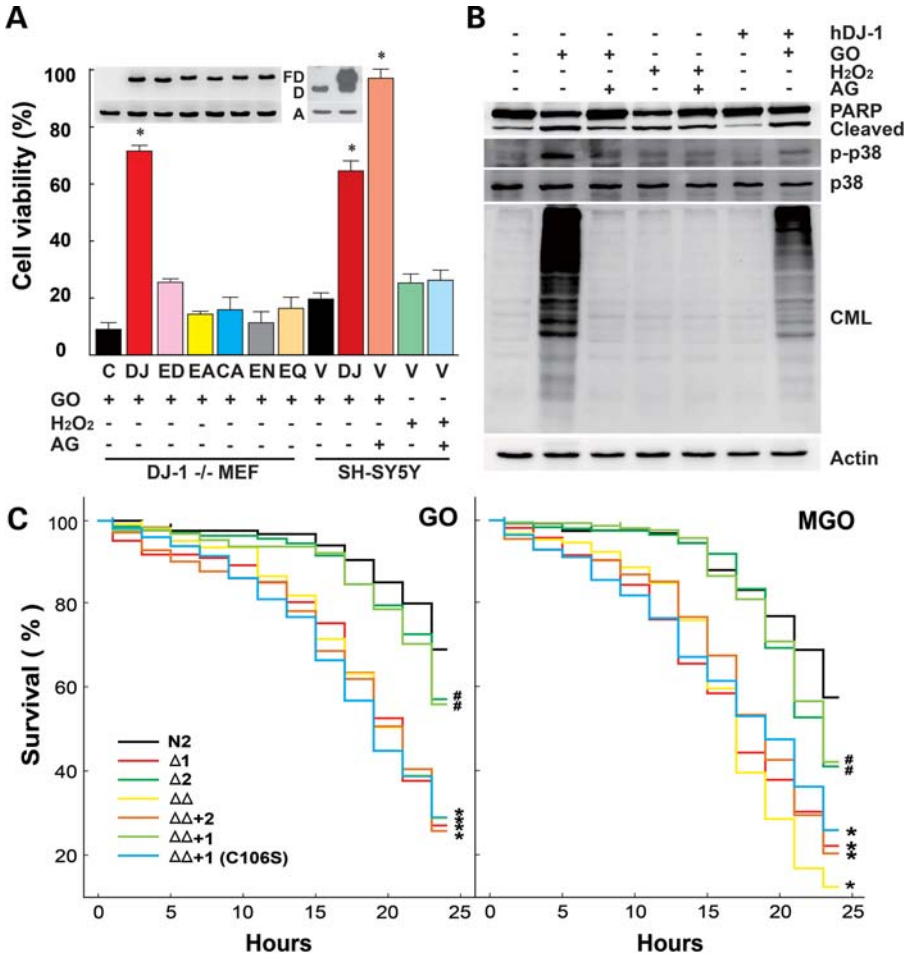

Figure 4. Protection of glyoxal-induced death by DJ-1. (**A**) MEF cells from the mDJ-1 KO mouse infected with murine stem cell virus (MSCV) containing hDJ-1 and its catalytic mutant forms were examined after treatment of 2 mM GO for 16 h. The viability of cells expressing DJ-1 was increased by 63%, compared with that of the control. SH-SY5Y cells were also treated with 2 mM GO for 16 h and tested for viability, showing that additional expression of DJ-1 increases ~45% of cell viability compared with that of the control. Co-treatment of 2 mM AG also increased cell viability of GO-treated cells, but not of H_2O_2-treated cells (300 μM hydrogen peroxide). Abbreviations: C, control; DJ, DJ-1; ED, E18D; EA, E18A; CA, C106A; EN, E18N; EQ, E18Q; V, vector; FD, Flag-DJ-1; D, DJ-1; A, actin with $n = 3$, $P < 0.001$ (*) by student's *t*-test. (**B**) Western blot of SH-SY5Y cells treated with 2 mM glyoxal and 300 μM H_2O_2 for 16 h. The presence of DJ-1 reduces CML, GO-induced PARP cleavage and phosphorylation of p38. (**C**) Viabilities of WT and *djr-1* mutant worms were observed by treating 200 mM GO or 100 mM MGO, showing differences in their survivals. Detailed genotypes are described in the Materials and Methods section. The loss of cDJR-1.1 turned out to be more effective in worm survival than that of cDJR-1.2. Worms injected with *djr-1.1* show rescuing effects: the experiments were replicated four times, and 35 worms were used for each experiment; $^{\#}P < 0.05$ and $^{*}P < 0.0001$ by the log-rank test.

intracellular level of carbonyl compounds has not yet been established. Our data indicating that the glyoxal effect, efficiently masked by AG treatment, does not elicit the detectible level of ROS increase appear to suggest that the role of DJ-1 in protecting glyoxal itself certainly exist, although we cannot completely rule out the possibility of an involvement of other DJ-1 functions, i.e. transcriptional activation (35) or molecular chaperone (36). Measuring worm viability upon exposure to glyoxals revealed that the loss of cDJR-1.1 results in considerably higher susceptibility *in vivo* to glyoxals than that of cDJR-1.2. This correlates with the results in Table 2, in which crude extracts from Δ*djr-1.2* worms show fairly high specific activity towards both MGO and GO, compared with that of Δ*djr-1.1* extracts. It is likely that cDJR-1.1 primarily contributes to protecting worms upon carbonyl stress, presumably due to its higher enzymatic activity and abundant expression in the intestine, while cDJR-1.2 does its job in more specific locations such as neuron and some other cells.

In rat hepatocytes and SH-SY5Y cells, it was reported that the treatment of GO or MGO resulted in collapsed mitochondrial membrane potential, depletion of GSH and an increase in ROS (29,37). The possibility of glyoxal as an inhibitor of the mitochondrial electron transport chain was also raised, providing a clue to understand DJ-1's role in carbonyl stress and mitochondrial dysfunction (38). Furthermore, recent studies emphasize the importance of DJ-1 in controlling mitochondria dynamics, in which an ablation of DJ-1 results in decreased mitochondrial potential, increase in mitochondria fragmentation, increase in ROS and induction of autophagic markers (39,40). While knockdown of other PD-associated genes such as *pink1* and *parkin* also result in mitochondrial dysfunction, DJ-1 has been suggested to serve independently in protecting

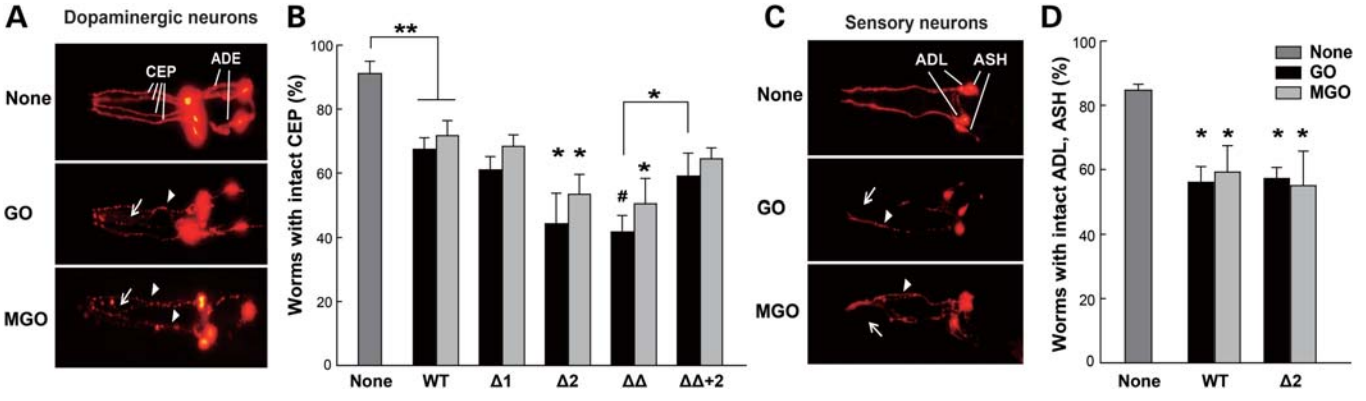

Figure 5. DJ-1 protection against glyoxal-induced neurodegeneration in *C. elegans*. Exposure to 50 mM GO for 2 days or 20 mM MGO for 1 day shows degeneration of (**A**) dopaminergic (CEP, ADE) and (**C**) sensory (ASH, ADL) neurons visualized with $P_{dat\text{-}1}$::mCherry and $P_{srb\text{-}6}$::mCherry injected worms, respectively, in which cells show blebbing (arrowhead), rounding and cell loss (arrow). (**B**) Worms with intact CEP were quantified by counting normal CEP (CEPDL, CEPDR, CEPVL and CEPVR) after treatment with the same conditions as (A). Loss of cDJR-1.2 results in significant CEP damage, while cDJR-1.1 affects little compared with that of the WT. (**D**) Neuronal viabilities of ASH and ADL sensory neurons were quantified by counting worms with intact neurons (ASHL, ASHR, ADLL and ADLR) in WT or Δ*djr-1.2* worms with the same conditions as in (C). Both strains show significant neuronal loss upon treatments of glyoxals, compared with that of non-treated control: the experiments were replicated four times, and 50 worms were used for each experiment; $^{*}P < 0.05$, $^{**}P < 0.01$ and $^{\#}P < 0.001$ by student's *t*-test after *post hoc* Bonferroni correction.

mitochondria from that of PINK1/Parkin (40,41). We believe that this mechanistic independence of DJ-1 action is due to its primary role as a glyoxalase scavenging reactive aldehydes.

MATERIALS AND METHODS

Protein purification

The cDNAs of *djr-1.1*, *djr-1.2*, DJ-1β, mDJ-1, hDJ-1 and their mutants were cloned into pET21a/pET15b vectors, which express N-term 6xHis-tagged cDJR-1.1 and C-term 6xHis-tagged cDJR-1.2, DJ-1β, mDJ-1 and hDJ-1. The cloned vectors were transformed into *E. coli* BL21(DE3), which were grown at 37°C in LB broth containing 0.1 mg/ml of ampicillin until the OD_{600} reached 0.4. Isopropyl-β-D-thiogalactoside (IPTG, 0.25 mM) was then added to over-produce protein, and cells were further incubated at 37°C for 4 h. After centrifugation, cells were resuspended in lysis buffer (50 mM NaH_2PO_4, 300 mM NaCl, 10 mM imidazole, pH 8.0) containing 14.3 mM β-mercaptoethanol and 0.5 mM phenylmethylsulfonylfluoride, followed by sonication and centrifugation (16 000*g*) at 4°C for 30 min. The supernatant was loaded onto the Ni^{2+}-NTA column, and the protein was eluted with 10–250 mM imidazole gradient. The purified proteins were subjected to dialysis using 100 mM Na_3PO_4 (pH 6.0) buffer.

^{1}H-NMR and HPLC analysis

For the detection of enzyme product, purified human DJ-1 was reacted with 3 mM MGO or 5 mM GO in 100 mM potassium phosphate buffer (pH 6.8) for 30 min, and subjected to NMR experiment. Measurements were made in 600 μl solution with 10% D_2O as a locking substance. The proton NMR was carried out using short pulse width (3 μs) and long relaxation delay (5 s) for quantitative analysis. For detecting reaction products of cDJR-1.1/1.2, 10 μl of 5 M PCA was added to 90 μl of the reaction mixture, which was centrifuged (16 000*g*) and filtered through polyvinylidene fluoride membranes (pore size of 0.2 μm). Twenty microliter of the filtered samples were subjected to chromatographic analysis with HPLC equipped with the LC-20AB pump, SPD-20A UV monitor and a SIL-20A auto sampler (Shimadzu). A 250 mm × 4.6 mm stainless steel Prevail C18 column (Alltech, USA) was used with the flow rate of 1 ml/min and with acetonitrile/10 mM H_3PO_4 buffer (pH 2.5) as a mobile phase. Both lactic and glycolic acids were detected at 210 nm at room temperature.

Enzyme activity

One hundred micrograms of purified DJ-1s (50 μg in the case of hDJ-1) in 100 mM Na_3PO_4 buffer (pH 6.0 for cDJR-1.1, cDJR-1.2 and pH 6.8 for others) were added with various concentrations of glyoxals in a total reaction volume of 500 μl. The reaction was proceeded at 45°C for predetermined lengths of time, and stopped by adding 90 μl of 0.1% 2,4-dinitrophenylhydrazine (DNPH) solution in 210 μl of H_2O. The solution was incubated for 15 min at room temperature, and 420 μl of 10% NaOH was added. After further incubation for 15 min, absorbance (570 nm for GO and 540 nm for MGO) was measured, and the initial velocities were used to obtain kinetic values. The Sigma-plot program was used to plot the results obtained with the Michaelis–Menten and Lineweaver–Burk equations. His-tagging to DJ-1 did not influence its enzymatic activity, since the same protein without a tag exhibited similar degree of enzymatic activity (unpublished data). Specific activities of worm/mouse extracts were measured with the same assay method for 2 mg of each samples by incubating with 10/8 mM GO at 22/37°C, respectively. One unit of the specific activity was defined as the amount of enzyme used to convert 1 μmol substrate per minute. Measurement of glyoxalase I activity was carried out with 10 mM GO, 10 mM GSH and 1 mg of tissue extract in 100 mM Na_3PO_4 buffer (pH 7.4), which were incubated for 10 min at RT to form S-2-hydroxyethylglutathione that was measured at 240 nm.

Cell culture and viability assay

MEFs were prepared from E13.5 embryos of DJ-1 knockout mouse. DJ-$1^{-/-}$ MEFs were infected with retroviruses to express WT and mutant DJ-1s (E18D, E18A and C106A). The Flag-tagged WT and mutant DJ-1s contained in pMSCV (murine stem cell virus) were transfected to HEK-293T using polyethyleneimine (PEI, sigma). After 2 days, culture supernatant containing retroviruses were harvested and used to infect DJ-1 −/− MEFs with 3 μg/ml polybrene. The infected MEFs were selected with 2 μg/ml puromycin and maintained for further use. The human SH-SY5Y cells were transfected with the Flag-tagged WT DJ-1 using lipofectamine 2000 and selected with 500 μg/ml of G418. Stable clones were picked, grown and cultured in a humidified atmosphere with 5% CO_2 at 37°C. The cells were cultured in Dulbecco's modified Eagle's medium (DMEM) with 10% fetal bovine serum, 100 units/ml of penicillin and 100 μg/ml of streptomycin (Hyclone).

The infected MEFs were cultured in 96-well plates, adhered for 24 h and treated with 2 mM GO in DMEM for 16 h, washed with phosphate buffered saline (PBS) and added with a mixture of 90 μl DMEM (without phenol red, due to fluorescence interference) plus 10 μl Prestoblue (Invitrogen) per well, following the manufacturer's protocols. The fluorescence was measured using Infinite M200 (Tecan) with excitation at 560 nm and emission at 590 nm. The SH-SY5Y stable cell lines were treated with 2 mM GO or 300 μM H_2O_2, with or without 2 mM AG (sigma) in DMEM for 16 h, and cell viability was measured using Prestoblue as described above.

ROS measurement

To determine the levels of intracellular ROS in SH-SY5Y cells, we used fluorescent dye, CM-H_2DCF-DA (Invitrogen), which is passively permeant to cells, whose acetate groups are hydrolyzed by intracellular esterases. Adducts formed with intracellular ROS generate fluorescent CM-DCF. The SH-SY5Y cells (with the vector constructs) cultured 24 h on dishes were incubated with 10 μM CM-H_2DCFDA for 30 min at 37°C. The cells were then treated with 300 μM H_2O_2 or 2 mM GO in DMEM for 30 min at 37°C. After washing with PBS, intracellular ROS levels were analyzed with FACS (LSR II, BD Biosciences). For fluorescence microscopy (Olympus IX71), cover slips contained in 12-well plates were coated with poly-L-lysines. ROS levels were observed with 10× objective and analyzed using DeltaVision software (Applied Precision Inc.).

Immunoblotting

For immunoblotting, SH-SY5Y cells were harvested and lysed in radioimmunoprecipitation assay buffer (20 mM Tris–HCl, pH 7.5, 100 mM NaCl, 1 mM EDTA, 2 mM EGTA, 1 mM Na_3VO_4, 50 mM β-glycerophosphate, 50 mM NaF, 1% Triton X-100 and protease inhibitor cocktail). The lysates were separated by SDS–PAGE and transferred to a nitrocellulose membrane. The membranes were blocked for 2 h in 5% skim milk in TBS-Tween-20 at room temperature, followed by incubation at 4°C for overnight with antisera against DJ-1 (Lab work), Actin (Sigma), Nε-CML (R&D systems), PARP, phospho-p38 or p38 (Cell signaling). After washing three times, membranes were incubated with horseradish peroxidase-conjugated secondary antibodies in TBS-Tween-20. The proteins were developed and visualized using LAS-4000 (Fujifilm).

Caenorhabditis elegans strains and their maintenance

Caenorhabditis elegans strains were cultured according to the standard methods (42) and fed on mutant bacteria MG1655 Δ*hchA* Δ*yafB* Δ*yqhD*, which are unable to detoxify glyoxals due to deletions in glyoxalse III, AKR and aldehyde reductase. N2 Bristol was used as a WT, from which *djr-1.1*(*tm918*), *djr-1.2*(*tm1346*), HO1087 (*djr-1.1*(*tm918*)II; *djr-1.2*(*tm1346*)V) were originated. Transgenic lines used in viability assay contain promoters specific for *djr* genes fused to GFP, $P_{djr\text{-}1.1}$::*djr-1.1*::*gfp* and $P_{djr\text{-}1.2}$::*gfp*::*djr-1.2*, whose polymerase chain reaction (PCR) products were microinjected into the gonad of young adult (HO1087). Abbreviations of genotypes are as follows: Δ1, *djr-1.1*(*tm918*); Δ2, *djr-1.2*(*tm1346*); ΔΔ, HO1087; ΔΔ+1, *djr-1.1*;*djr-1.2* plus $P_{djr\text{-}1.1}$::*djr-1.1*::*gfp*; ΔΔ+2, *djr-1.1*;*djr-1.2* plus $P_{djr\text{-}1.2}$::*gfp*::*djr-1.2*; ΔΔ+1(C106S), *djr-1.1*;*djr-1.2* plus P*djr-1.1*::*djr-1.1*(*C106S*)::*gfp*. Strains used in neuronal degeneration assay were generated by microinjecting $P_{dat\text{-}1}$::mCherry into WT and cDJR knockout strains described above.

Construction of transgenic worms

Translational fusion of *djr-1.1* and *gfp* ($P_{djr\text{-}1.1}$::*djr-1.1*::*gfp*) were created by PCR. Four kilobase pair upstream of the initiation codon to the end of the third exon of *djr-1.1* was amplified from *C. elegans* genomic DNA and fused with amplified *gfp* from pPD95.79. $P_{djr\text{-}1.2}$::*gfp*::*djr-1.2* were created using the same method described above, except for an extra 2 kb upstream of the initiation codon. $P_{dat\text{-}1}$::mCherry and $P_{srb\text{-}6}$::mCherry were also made by connecting 1 kb regions upstream of *dat-1* and *srb-6* start codons with mCherry, respectively, which were amplified from pKA384 (from SJ. Lee, Pohang University of Science and Technology). The PCR constructs were microinjected into WT and mutant hermaphrodites, and transgenic lines were confirmed by single-worm PCR, using primers recognizing *djr-1.1* and *1.2* sequences.

Lifespan and viability assays for worms

For measuring lifespan, 1-day-old adult worms were transferred onto nematode growth medium (NGM) plates, and survivals of worms were checked daily. For assaying viability upon GO/MGO treatment, 1-day-old adult worms were transferred to NGM plates containing 200 mM GO/100 mM MGO, and survival of worms was checked every 2 h. Worms were considered dead if not responding to touch with a platinum wire. Several drops of 10 mg/ml palmitic acid (dissolved in ethanol) were placed on the edge of the plates and dried to create a physical barrier that can prevent worms from crawling out NGM plates.

Preparation of mouse tissues and worm extract

For measuring enzyme activity, liver and brain from mice were removed and added with 100 mM Na_3PO_4 buffer (pH

6.8) containing 5 mM DTT. The samples were homogenized, sonicated and centrifuged (222 592*g*) at 4°C, and the supernatant was subject to dialysis with 100 mM Na_3PO_4 buffer (pH 6.8) containing 5 mM DTT. Worms were grown in liquid S medium [1 l of S-basal (5.85 g NaCl, 1 g K_2HPO_4, 6 g KH_2PO_4, 1 ml cholesterol (5 mg/ml in ethanol) and H_2O up to 1 l) plus 10 ml of 1 M KCO_3, pH 6.0, 10 ml of trace metal solution, 3 ml of 1 M $CaCl_2$ and 3 ml of 1 M $MgSO_4$] containing bacteria for food. After incubating for 6 days, worms were harvested, washed and sonicated with 100 mM Na_3PO_4 buffer (pH 6.0) containing 1 mM DTT and protease inhibitor cocktail. The sonicated samples were centrifuged (16 000*g*) at 4°C, and the supernatant was subject to dialysis with 100 mM Na_3PO_4 buffer (pH 6.0), containing 1 mM DTT in order to eliminate co-factors that may complicate an involvement of other glyoxal detoxifying activities. Protein concentrations (μg/μl) of the mouse and worm extracts were determined by Bradford assay. One microliter of the sample extract was added to 99 μl of H_2O plus 1 ml of Bradford solution (BioRad) and vortexed, and the absorbance was measured at 595 nm. The protein standard was obtained by serially diluting bovine serum albumin (BSA), in which A_{595} = (sample concentration − 0.0052)/0.0818 was used for calculation.

Immunostaining and microscopy

COS7 cells were cultured on a cover glass, being placed inside a 12-well plate, with high glucose DMEM plus 10% FBS. Flag-tagged *djr-1.1* and *djr-1.2* cloned in pDK-FLAG1 were transfected into cells using PEI solution, and immunostaining was performed after 24 h of transfection. For immunostaining, cells were treated with mitotracker for 30 min and washed with ice-cold 1× PBS. Cells were then treated with 2% paraformaldehyde for 15 min at RT, washed with 0.1% PBS-Triton X-100 (PBST), and treated with 0.5% PBST for 5 min at RT. After washing with 0.1% PBST, cells were incubated with blocking solution (0.1% PBST, 3% BSA and 1:100 of goat normal serum) for 1 h at 37°C, followed by a treatment with anti-Flag M2 (Sigma) in blocking solution (1:200) for 1 h at RT. After washing three times with 0.1% PBST, cells were further incubated with anti-mouse-FITC (Sigma) at dark for 1 h at RT and washed three times with 0.1% PBST. Washed cells were mounted on a slide glass using DAPI-containing vectashield (Vector Laboratories), and images of the immunostained cells were captured with Zeiss 510 confocal microscope. For imaging GFP-expressing and DiI-stained worms, organisms were paralyzed by placing on a 2% agar pad in a drop of 12.5% sodium azide and observed under fluorescence microscopy.

Antibody production

Full-length cDNAs of *djr-1.1* and *djr-1.2* were cloned into vector pET21a and expressed in *E. coli* BL21(DE3). Proteins were purified using Ni^{2+}-NTA resin as described above, and 60 μg of protein was injected into guinea pigs every week. After 10th injection, polyclonal antiserum was obtained by taking supernatant after incubating the blood for 1 h at 37°C and centrifugation (16 000*g*) at 4°C.

Observation of neuronal degeneration

Age-synchronized L3 worms were treated with 50 mM GO (2 days) or 20 mM MGO (1 day) in 1× PBS containing bacteria as food. The worm solution was placed in a micro test tube with a total volume of 1 ml and incubated at 20°C. For 6-OHDA experiment, L3 worms were treated with 2 mM 6-OHDA plus 5 mM ascorbic acid for 2 days. In order to prevent worms from drowning, worm and chemical-containing micro test tubes were constantly rotated using Rotamix RM1. Worms were then poured onto NGM plates and incubated for additional 12 h for recovery. Live worms were paralyzed by placing worms on a 2% agar pad in a drop of 12.5% sodium azide, and worms with normal CEP neurons were counted under fluorescence microscopy. Neurons with 'dendrite blebbing', 'cell body rounding', or 'cell body loss' were considered as affected.

Statistical analysis

All statistical analysis was performed using the Prism software. Two-tailed student's *t*-test was used to assess differences between control and other groups, and the log-rank test was used for survival analysis.

SUPPLEMENTARY MATERIAL

Supplementary Material is available at *HMG* online.

ACKNOWLEDGEMENTS

We thank In-sook Kim and Bum-chan Min for performing ^{1}H-NMR analysis and S. J. Lee for providing vector constructs. The authors also thank Dong-Wook Choi for helpful comments.

Conflict of Interest statement. None declared.

FUNDING

This work was supported by grants from Korea Institute of Planning and Evaluation for Technology in food, agriculture, forestry and fisheries to C. Park and from Inha University to J. Kim. K. Baek was funded by the National Research Foundation of Korea (NRF) grant (Grant No. 2011-0007189).

REFERENCES

1. Bonifati, V., Rizzu, P., van Baren, M.J., Schaap, O., Breedveld, G.J., Krieger, E., Dekker, M.C., Squitieri, F., Ibanez, P., Joosse, M. *et al.* (2003) Mutations in the DJ-1 gene associated with autosomal recessive early-onset parkinsonism. *Science*, **299**, 256–259.
2. Nagakubo, D., Taira, T., Kitaura, H., Ikeda, M., Tamai, K., Iguchi-Ariga, S.M. and Ariga, H. (1997) DJ-1, a novel oncogene which transforms mouse NIH3T3 cells in cooperation with ras. *Biochem. Biophys. Res. Commun.*, **231**, 509–513.
3. Canet-Aviles, R.M., Wilson, M.A., Miller, D.W., Ahmad, R., McLendon, C., Bandyopadhyay, S., Baptista, M.J., Ringe, D., Petsko, G.A. and Cookson, M.R. (2004) The Parkinson's disease protein DJ-1 is neuroprotective due to cysteine-sulfinic acid-driven mitochondrial localization. *Proc. Natl Acad. Sci. USA*, **101**, 9103–9108.

4. Guzman, J.N., Sanchez-Padilla, J., Wokosin, D., Kondapalli, J., Ilijic, E., Schumacker, P.T. and Surmeier, D.J. (2010) Oxidant stress evoked by pacemaking in dopaminergic neurons is attenuated by DJ-1. *Nature*, **468**, 696–700.
5. Meulener, M., Whitworth, A.J., Armstrong-Gold, C.E., Rizzu, P., Heutink, P., Wes, P.D., Pallanck, L.J. and Bonini, N.M. (2005) Drosophila DJ-1 mutants are selectively sensitive to environmental toxins associated with Parkinson's disease. *Curr. Biol.*, **15**, 1572–1577.
6. Taira, T., Saito, Y., Niki, T., Iguchi-Ariga, S.M., Takahashi, K. and Ariga, H. (2004) DJ-1 has a role in antioxidative stress to prevent cell death. *EMBO Rep.*, **5**, 213–218.
7. Martinat, C., Shendelman, S., Jonason, A., Leete, T., Beal, M.F., Yang, L., Floss, T. and Abeliovich, A. (2004) Sensitivity to oxidative stress in DJ-1-deficient dopamine neurons: an ES- derived cell model of primary Parkinsonism. *PLoS Biol.*, **2**, e327.
8. Ved, R., Saha, S., Westlund, B., Perier, C., Burnam, L., Sluder, A., Hoener, M., Rodrigues, C.M., Alfonso, A., Steer, C. *et al.* (2005) Similar patterns of mitochondrial vulnerability and rescue induced by genetic modification of alpha-synuclein, parkin, and DJ-1 in *Caenorhabditis elegans*. *J. Biol. Chem.*, **280**, 42655–42668.
9. Harrington, A.J., Hamamichi, S., Caldwell, G.A. and Caldwell, K.A. (2010) *C. elegans* as a model organism to investigate molecular pathways involved with Parkinson's disease. *Dev. Dyn.*, **239**, 1282–1295.
10. Thornalley, P.J., Langborg, A. and Minhas, H.S. (1999) Formation of glyoxal, methylglyoxal and 3-deoxyglucosone in the glycation of proteins by glucose. *Biochem. J.*, **344**, 109–116.
11. Munch, G., Luth, H.J., Wong, A., Arendt, T., Hirsch, E., Ravid, R. and Riederer, P. (2000) Crosslinking of alpha-synuclein by advanced glycation endproducts—an early pathophysiological step in Lewy body formation? *J. Chem. Neuroanat.*, **20**, 253–257.
12. Brownlee, M. (1995) Advanced protein glycosylation in diabetes and aging. *Annu. Rev. Med.*, **46**, 223–234.
13. Luth, H.J., Ogunlade, V., Kuhla, B., Kientsch-Engel, R., Stahl, P., Webster, J., Arendt, T. and Munch, G. (2005) Age- and stage-dependent accumulation of advanced glycation end products in intracellular deposits in normal and Alzheimer's disease brains. *Cereb. Cortex*, **15**, 211–220.
14. Kikuchi, S., Shinpo, K., Moriwaka, F., Makita, Z., Miyata, T. and Tashiro, K. (1999) Neurotoxicity of methylglyoxal and 3-deoxyglucosone on cultured cortical neurons: synergism between glycation and oxidative stress, possibly involved in neurodegenerative diseases. *J. Neurosci. Res.*, **57**, 280–289.
15. Thornalley, P.J. (1990) The glyoxalase system: new developments towards functional characterization of a metabolic pathway fundamental to biological life. *Biochem. J.*, **269**, 1–11.
16. Vander Jagt, D.L., Robinson, B., Taylor, K.K. and Hunsaker, L.A. (1992) Reduction of trioses by NADPH-dependent aldo-keto reductases. Aldose reductase, methylglyoxal, and diabetic complications. *J. Biol. Chem.*, **267**, 4364–4369.
17. Misra, K., Banerjee, A.B., Ray, S. and Ray, M. (1995) Glyoxalase III from Escherichia coli: a single novel enzyme for the conversion of methylglyoxal into D-lactate without reduced glutathione. *Biochem. J.*, **305**, 999–1003.
18. Subedi, K.P., Choi, D., Kim, I., Min, B. and Park, C. (2011) Hsp31 of Escherichia coli K-12 is glyoxalase III. *Mol. Microbiol.*, **81**, 926–936.
19. Cha, S.S., Jung, H.I., Jeon, H., An, Y.J., Kim, I.K., Yun, S., Ahn, H.J., Chung, K.C., Lee, S.H., Suh, P.G. *et al.* (2008) Crystal structure of filamentous aggregates of human DJ-1 formed in an inorganic phosphate-dependent manner. *J. Biol. Chem.*, **283**, 34069–34075.
20. Odani, H., Shinzato, T., Matsumoto, Y., Usami, J. and Maeda, K. (1999) Increase in three alpha,beta-dicarbonyl compound levels in human uremic plasma: specific in vivo determination of intermediates in advanced Maillard reaction. *Biochem. Biophys. Res. Commun.*, **256**, 89–93.
21. Kurz, A., Rabbani, N., Walter, M., Bonin, M., Thornalley, P., Auburger, G. and Gispert, S. (2011) Alpha-synuclein deficiency leads to increased glyoxalase I expression and glycation stress. *Cell Mol. Life Sci.*, **68**, 721–733.
22. Xue, M., Rabbani, N., Momiji, H., Imbasi, P., Anwar, M.M., Kitteringham, N., Park, B.K., Souma, T., Moriguchi, T., Yamamoto, M. *et al.* (2012) Transcriptional control of glyoxalase 1 by Nrf2 provides a stress-responsive defence against dicarbonyl glycation. *Biochem. J.*, **443**, 213–222.
23. Clements, C.M., McNally, R.S., Conti, B.J., Mak, T.W. and Ting, J.P. (2006) DJ-1, a cancer- and Parkinson's disease-associated protein, stabilizes the antioxidant transcriptional master regulator Nrf2. *Proc. Natl Acad. Sci. USA*, **103**, 15091–15096.
24. Niki, T., Takahashi-Niki, K., Taira, T., Iguchi-Ariga, S.M. and Ariga, H. (2003) DJBP: a novel DJ-1-binding protein, negatively regulates the androgen receptor by recruiting histone deacetylase complex, and DJ-1 antagonizes this inhibition by abrogation of this complex. *Mol. Cancer Res.*, **1**, 247–261.
25. Bandopadhyay, R., Kingsbury, A.E., Cookson, M.R., Reid, A.R., Evans, I.M., Hope, A.D., Pittman, A.M., Lashley, T., Canet-Aviles, R., Miller, D.W. *et al.* (2004) The expression of DJ-1 (PARK7) in normal human CNS and idiopathic Parkinson's disease. *Brain*, **127**, 420–430.
26. Zhang, L., Shimoji, M., Thomas, B., Moore, D.J., Yu, S.W., Marupudi, N.I., Torp, R., Torgner, I.A., Ottersen, O.P., Dawson, T.M. *et al.* (2005) Mitochondrial localization of the Parkinson's disease related protein DJ-1: implications for pathogenesis. *Hum. Mol. Genet.*, **14**, 2063–2073.
27. Morcos, M., Du, X., Pfisterer, F., Hutter, H., Sayed, A.A., Thornalley, P., Ahmed, N., Baynes, J., Thorpe, S., Kukudov, G. *et al.* (2008) Glyoxalase-1 prevents mitochondrial protein modification and enhances lifespan in *Caenorhabditis elegans*. *Aging Cell*, **7**, 260–269.
28. Nass, R., Hall, D.H., Miller, D.M. 3rd and Blakely, R.D. (2002) Neurotoxin-induced degeneration of dopamine neurons in *Caenorhabditis elegans*. *Proc. Natl Acad. Sci. USA*, **99**, 3264–3269.
29. Shangari, N. and O'Brien, P.J. (2004) The cytotoxic mechanism of glyoxal involves oxidative stress. *Biochem. Pharmacol.*, **68**, 1433–1442.
30. Inden, M., Taira, T., Kitamura, Y., Yanagida, T., Tsuchiya, D., Takata, K., Yanagisawa, D., Nishimura, K., Taniguchi, T., Kiso, Y. *et al.* (2006) PARK7 DJ-1 protects against degeneration of nigral dopaminergic neurons in Parkinson's disease rat model. *Neurobiol. Dis.*, **24**, 144–158.
31. Zhou, W. and Freed, C.R. (2005) DJ-1 up-regulates glutathione synthesis during oxidative stress and inhibits A53T alpha-synuclein toxicity. *J. Biol. Chem.*, **280**, 43150–43158.
32. Wilson, M.A., Ringe, D. and Petsko, G.A. (2005) The atomic resolution crystal structure of the YajL (ThiJ) protein from *Escherichia coli*: a close prokaryotic homologue of the Parkinsonism-associated protein DJ-1. *J. Mol. Biol.*, **353**, 678–691.
33. Yanagida, T., Tsushima, J., Kitamura, Y., Yanagisawa, D., Takata, K., Shibaike, T., Yamamoto, A., Taniguchi, T., Yasui, H., Taira, T. *et al.* (2009) Oxidative stress induction of DJ-1 protein in reactive astrocytes scavenges free radicals and reduces cell injury. *Oxid. Med. Cell Longev.*, **2**, 36–42.
34. Pham, T.T., Giesert, F., Rothig, A., Floss, T., Kallnik, M., Weindl, K., Holter, S.M., Ahting, U., Prokisch, H., Becker, L. *et al.* (2010) DJ-1-deficient mice show less TH-positive neurons in the ventral tegmental area and exhibit non-motoric behavioural impairments. *Genes Brain Behav.*, **9**, 305–317.
35. Kahle, P.J., Waak, J. and Gasser, T. (2009) DJ-1 and prevention of oxidative stress in Parkinson's disease and other age-related disorders. *Free Radic. Biol. Med.*, **47**, 1354–1361.
36. Shendelman, S., Jonason, A., Martinat, C., Leete, T. and Abeliovich, A. (2004) DJ-1 is a redox-dependent molecular chaperone that inhibits alpha-synuclein aggregate formation. *PLoS Biol.*, **2**, e362.
37. de Arriba, S.G., Stuchbury, G., Yarin, J., Burnell, J., Loske, C. and Munch, G. (2007) Methylglyoxal impairs glucose metabolism and leads to energy depletion in neuronal cells—protection by carbonyl scavengers. *Neurobiol. Aging*, **28**, 1044–1050.
38. Rabbani, N. and Thornalley, P.J. (2008) Dicarbonyls linked to damage in the powerhouse: glycation of mitochondrial proteins and oxidative stress. *Biochem. Soc. Trans.*, **36**, 1045–1050.
39. Irrcher, I., Aleyasin, H., Seifert, E.L., Hewitt, S.J., Chhabra, S., Phillips, M., Lutz, A.K., Rousseaux, M.W., Bevilacqua, L., Jahani-Asl, A. *et al.* (2010) Loss of the Parkinson's disease-linked gene DJ-1 perturbs mitochondrial dynamics. *Hum. Mol. Genet.*, **19**, 3734–3746.
40. Thomas, K.J., McCoy, M.K., Blackinton, J., Beilina, A., van der Brug, M., Sandebring, A., Miller, D., Maric, D., Cedazo-Minguez, A. and Cookson, M.R. (2011) DJ-1 acts in parallel to the PINK1/parkin pathway to control mitochondrial function and autophagy. *Hum. Mol. Genet.*, **20**, 40–50.
41. Hao, L.Y., Giasson, B.I. and Bonini, N.M. (2010) DJ-1 is critical for mitochondrial function and rescues PINK1 loss of function. *Proc. Natl Acad. Sci. USA*, **107**, 9747–9752.
42. Brenner, S. (1974) The genetics of *Caenorhabditis elegans*. *Genetics*, **77**, 71–94.